International Journal of Recent Technology and Engineering (IJRTE)
ISSN: 2277-3878 (Online), Volume-10 Issue-5, January 2022

Qualitative Analysis of Magnetic Moment in Ba_xTiO_3 - $Ni_xFe_{3-x}O_4$ Nanocomposite Synthesized by Novel low Temperature Technique

Ashwin Sudhakaran, Allwin Sudhakaran, E. Siva Senthil

Abstract: ***A novel low temperature preparation technique (<500ºC) is employed for synthesizing nanoscale Barium Titanate -Nickel ferrite composites, where the particle size is controllable. Two different ratios of hard and soft site composites (BTO-NFO 80:20, BTO-NFO 70:30) are synthesized and characterized to study their unique structural, morphological and magnetic properties. The structural refinement studies using XRD data showed 43 % of hard phase (anorthic structure) and 57% of soft phase (Cubic Structure) for BTO-NFO 80:20 and similarly 76% of hard phase and 24% of soft phase in the BTO-NFO 70:30 composite respectively. The SEM and EDAX are used to identify smaller particles of 10 nm using histogram and their sample purity. The VSM analysis at room temperature shows superparamagnetic behavior within the soft ferro magnet with maximum retentivity 2.39 emu/g and saturation magnetization, 10.71 emu/g stating that the composites can be used for various biological applications like drug delivery, hyperthermia, MRI, etc. The ratio Mr/Ms is much less than 0.5, which states that multidomain grains or single domains are formed and the particle interaction is by magneto-static interaction confirming its superparamagnetic nature***

Key Words: ***Barium Titanate, Nickel ferrite, Nanocomposite, Superparamagnetic, Low Temperature, Magnetic Moment, Bandgap Energy, Coprecipitation, Sol Gel-Auto Combustion, Physical Mixing.***

I. INTRODUCTION

Multifunctional materials have brought greater interest to researchers for the last decade. Materials like Multiferroics and ferroics have the possibility of opening enormous applications in the field of magneto-electric materials, which can have two parallel properties at the same time. Such properties can exceed the traditional use of magneto-electric materials. These applications include the scope of controlling magnetic phase by electric fields to magnetically controlled ferroelectrics. A large number of theoretical, experimental and application-oriented publications were done in these multifunctional materials in the past years.

Manuscript received on November 20, 2020.
Revised Manuscript received on November 25, 2021.
Manuscript published on January 30, 2022.
* Correspondence Author
Ashwin Sudhakaran*, Department of Physics, Karpagam Academy of Higher Education, Coimbatore (Tamil Nadu), India.
Allwin Sudhakaran, Department of Physics, Karpagam Academy of Higher Education, Coimbatore, (Tamil Nadu), India.
E. Siva Senthil, Department of Physics, Karpagam Academy of Higher Education, Coimbatore, (Tamil Nadu), India. E-mail. sivasenthil.e@kahedu.edu.in

Multiferroics was also listed as the only one in top ten "Areas to study" in the field of Material Science in the upcoming years. Today such materials have expanded their properties and are also used for advanced electronic devices [1], [2]. These composites have magneto-electric coupling, which is the ability to control the magnetic phase under the influence of an electric field and vice versa [3]. Such materials can also be termed as Magneto-electric Multiferroics. It is to be noted that when two different phases coexist with each other as multiferroics, there is a dilution between the electric and magnetic phases. In recent periods different types of Multiferroic composites are reported [1]–[6]. It is to be noted that the preparation techniques play a significant role in achieving the desired properties of the final composite material. Though the future will need more such types of composite materials, there are some problems in synthesizing such multiferroics which need to be solved [4]. Besides research, multiferroics have potential applications as novel electronic memory devices, transducers, actuators, capacitive filters or inductive filters for telecommunication, magnetic field sensors, electric-write magnetic-read memory devices etc. [7]–[14]. Nano ferrites or nano-multiferroics have various applications in areas like noval storage devices, Nano-electric generators, ferro-fluids, microwave devices, antennas, magnetic refrigerators, heterogeneous catalysts, targeted drug delivery and as repulsion-suspension in levitated railway systems [14]–[16].

Among various ferroelectrics like Lead Titanate, Lead zirconium titanate, Barium Titanate, Rochelle salt etc, Barium titanate is used widely due to its less toxicity compared to lead based materials. These materials have high energy storage properties and are environmentally friendly in nature. It is believed that Barium titanate based ceramics can not only improve the electric energy storage performance but also be used in high level advance applications including advanced pulsed power capacitors, High electron mobility transistors, flexible polymer dye sensitized solar cell, photodetectors, tunable microwave devices, mid-infrared electro optical waveguide modulators etc. [17]–[22]. Nickel ferrite on the other hand are soft ferrite materials that are multifaceted having ferromagnetic properties with low eddy current loss, high electrochemical stability and low conductivity. They also show super paramagnetic behavior which can be used in applications including gas sensors, magnetic fluids, magnetic hyperthermia, battery catalysts, magnetic storage devices, microwave devices etc. [22]–[28].

More recently a biomechanical energy harvesting device has been fabricated by Hangzhou et al, using a pair of multiferroic laminates of high magneto-electro strictive properties [15]. With Barium titanate composite blended with PDMS (polydimethylsiloxane), Hajra et al constructed a hybrid nano-generator device that can generate a maximum electrical output of 320 V and 12μA [16]. Since previous research on barium titanate and nickel ferrite shows that the multiferroic behavior can be significantly improved by choosing appropriate synthesizing techniques, low temperature preparation techniques are used to prepare BTO-NFO nano composites of two different ratios, 80-20 and 70-30 respectively; and their enhanced magnetic properties are deliberated in this paper.

A. Preparation of Hard site material:

The composite material consists of two particles. One is the hard phase and another one is the soft phase in terms of its Ferro properties. The idea is to prepare a nanocomposite with barium titanate on the hard site and Nickel ferrite on the soft side. For the preparation of barium titanate particles the coprecipitation method is employed. At first a stoichiometric amount of Barium Chloride, Titanium tetrachloride and Oxalic acid are dissolved in deionized water which is magnetically stirred for 30 minutes. The solution is then left to settle down to form precipitate and the decanting process is carried out several times. Later the precipitate is heated on a hot plate at 80-degree Celsius to form powdered barium titanate particles. The particles are later crushed in motor pistol and then collected

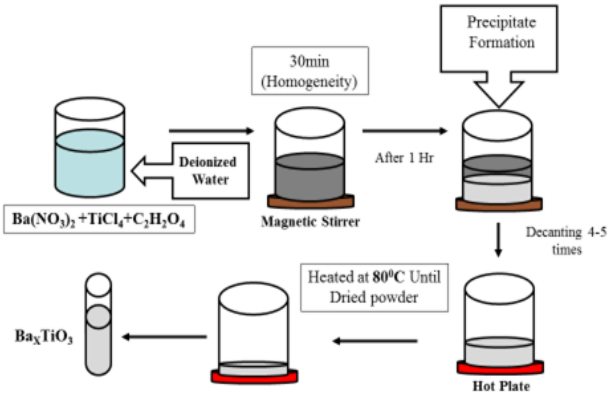

Figure 1. Synthesis of Barium Titanate by co-precipitation Method.

B. Preparation of Soft site material:

The Soft side Nickel ferrite is synthesized by Sol gel auto combustion technique. In deionized water, the stoichiometric amount of Nickel nitrate, ferric nitrate and citric acid is dissolved. The solution is magnetically stirred and heated until the solution turns into the preferred gel condition, that is further heated at a low temperature in a hot plate until it is self-combusted to form dark brown powders. The precursor powder is then annealed at 400°C for 6 hours. The final Nickel ferrite powders are collected.

C. Preparation of Nanocomposite material:

For preparation of nanocomposites, a physical mixing route is employed. 80 and 70% weight ratio of as-prepared barium titanate are mixed with 20 and 30% weight ratio of as-prepared nickel ferrite particles which are grinded for 1 hour by using motor and pistol. Thus, the composites are taken in two different ratios of 80:20 and 70:30 respectively and are named as BTO-NFO 80-20 and BTO-NFO 70-30. These two sample powders are further given for characterization.

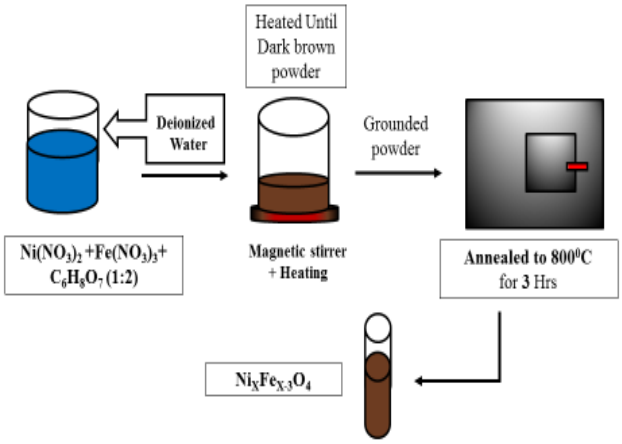

Figure 2. Synthesis of Nickel Ferrite by Sol-Gel auto-combustion Method.

II. EXPERIMENTAL TECHNIQUES:

The prepared nanocomposites are given for the following characterization. For Structural analysis, 3rd generation Empyrean X-ray diffractometer, Malvern Panalytical with Cu Kα (λ=1.540598 Å) radiation is used. Morphology along with their particle size distribution are analyzed using Scanning Electron Microscopy (SEM) Jeol JSM 6390model equipped with EDX for determination of chemical composition and weight percentage of chemicals. For Magnetic studies, 7407 lakeshore- Vibrating sample magnetometer calibrated to 1.5 Tesla at room temperature is used to find the magnetic moment of BTO-NFO composites.

III. RESULTS AND DISCUSSIONS:

A. Structural analysis:

The structural analyses of the samples (BTO-NFO 80-20 and BTO-NFO 70-30) are carried out using XRD. All peaks are indexed in accordance with matching JCPDS card number,40-0405 for BTO & 88-0380 for NFO. Barium titanate is found to have anorthic (triclinic) structure whereas Nickel ferrite possesses Cubic structure. All the lattice parameters a, b, c, α, β and γ were found to be similar to pure BTO & NFO JCPDS card numbers. The lattice parameters are tabulated and it is observed that except c all other lattice parameters increase with increase in the soft site concentration. The intensity of the peak increases with an increase in the hard site content. Also, when compared with the BTO-NFO 70-30 sample, sharper and new defined peaks are observed in the BTO-NFO 80-20 composite. This means that new peaks are found with high concentrations of the hard site materials. The lattice parameter and cell volume are calculated and tabulated as shown in Table 1.

Published By:
Blue Eyes Intelligence Engineering
and Sciences Publication (BEIESP)

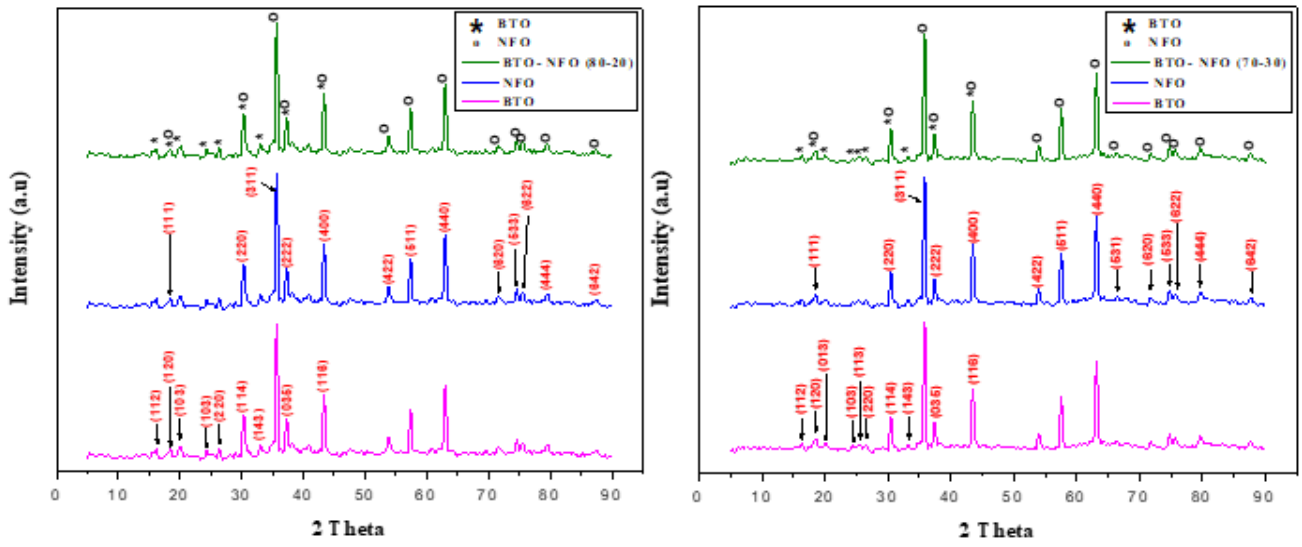

Figure 3. The XRD patterns for BTO-NFO 80-20 and 70-30 respectively.

Further to find the average crystallite size of the prepared nanocomposite, Scherrer's equation is used considering the diffraction peaks of Higher intensities for BTO and Highest peak (311) for NFO.

Table 1: Comparison of standard and calculated lattice parameter and cell volume for BTO-NFO 80-20 and BTO-NFO 70-30.

	a	b	c	α	β	γ	Cell Vol.
Standard Value (BTO)	7.471	14.08	14.344	89.94	79.43	84.45	1476.20
Standard Value (NFO)	8.335	-	-	90	90	90	579.11
Calculated Value BTO-NFO 80-20							
BTO	**7.75904**	**12.27372**	**12.84260**	**90.03665**	**74.02673**	**86.02760**	**1172.73**
NFO	**8.305567**	-	-	90	90	90	**573.0**
Calculated Value BTO-NFO 70-30							
BTO	**7.88895**	**12.49493**	**12.83136**	**90.92310**	**74.44412**	**88.92589**	**1217.97**
NFO	**8.330284**	-	-	90	90	90	**578.10**

Table 2: Average crystalline size of BTO-NFO nanocomposite calculated using Scherrer's equation.

		Peaks Taken	Range of Particles (nm)		Average size (nm)
			From	To	
BTO-NFO	**80-20**	Diffraction peaks of Higher intensities	19.24	30.77	25.44
	70-30		22.88	32.08	26.99

By substituting K=0.9 in the equation, D= k*λ/ (β*Cosθ), the resultant values are tabulated in table 2 where a smaller crystalline size of 19nm and 22 nm are observed in BTO-NFO 80-20 and BTO-NFO 70-30 nanocomposites respectively. In comparison, it is seen that the average crystallite size for BTO - NFO increases with the increase in soft site concentration in both cases of 80-20 and 70-30 samples. The structural refinement studies using XRD data showed 43 % of hard phase (anorthic structure) and 57% of soft phase (Cubic Structure) for BTO-NFO 80:20 and similarly 76% of hard phase and 24% of soft phase in the BTO-NFO 70:30 composite respectively.

IV. MORPHOLOGICAL ANALYSIS:

The SEM micrograph along with histograms of particle size distribution for both the samples are shown in figure 4 and 5. From the SEM image very dense microstructures were observed with average particle size less than 10nm. It is interesting to notice that the grain size is uniformly distributed throughout the sample. It is to be noted that the grain size obtained from SEM is smaller when compared to the crystalline size of the sample calculated from XRD analysis. The typical SEM micrograph and particle size distribution with histogram of BTO-NFO samples are shown in figures below. Dense microstructure has been observed from the SEM micrograph. It is very interesting that the grain sizes are uniformly distributed throughout the sample. All the samples have similar particle distribution (As shown below). The grain sizes obtained from SEM are smaller than the crystallite size calculated from the XRD analysis. It divulges the multiple crystallites or agglomerations in a single particle and form grains, which are separated by crystallographic grain boundaries inside the grains. A much Dissimilarities between crystallite size (from XRD analysis) and grain size (from SEM analysis) has been reported by another set of researchers [1], [2].

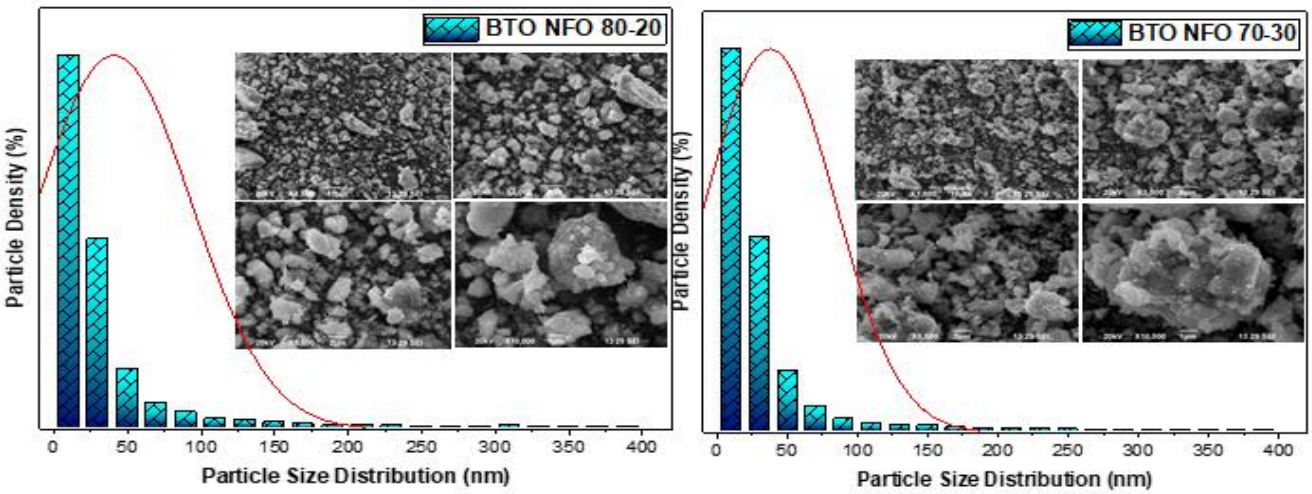

Figure 4. Typical SEM micrograph and particle size distribution with histogram of BTO-NFO 80-20 and of BTO-NFO 70-30 nanocomposite.

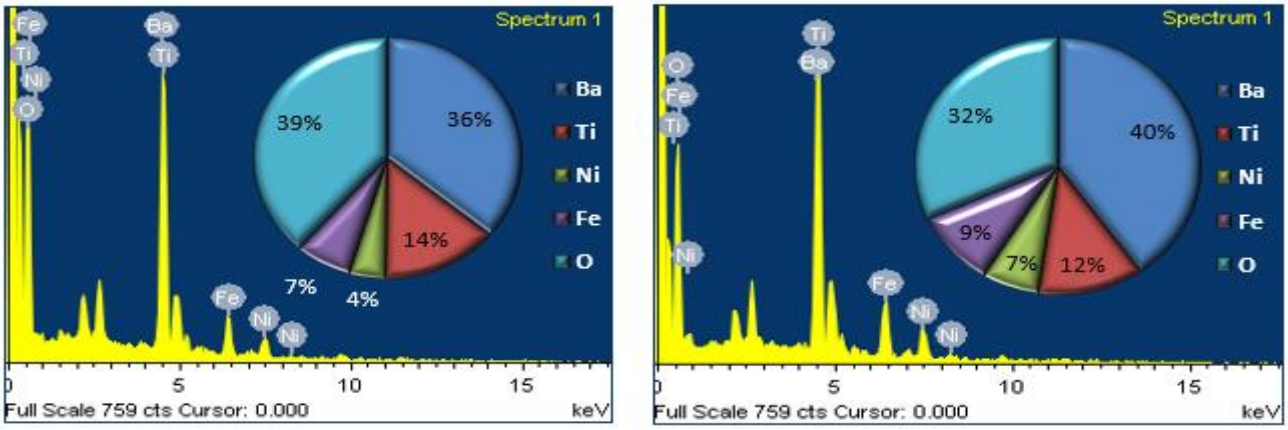

Figure 6. EDAX analysis for BTO-NFO reveals the presence of elements along with weight %.

It is stated that these are some typical characteristics of oxide-based materials which are the limitations of the XRD technique. The EDAX analysis was performed on the surface of the samples to determine its chemical compositions. The EDX spectrum (Figure 6) reveals the presence of Barium, Titanium, Nickel, Iron and Oxygen elements in $BaTiO_3$-$NiFe_2O_4$ in 80-20 and 70-30 samples respectively.

The quantitative data extracted from the EDX spectra are enlisted in table 3 and it confirmed that no element/s (impurity) is/are present in the composite sample other than Ba, Ti, Ni, Fe and O.

Table 3: Quantitative data extracted from the EDX spectra of BTO-NFO Nanocomposite.

Sample	Element	80-20			70-30		
		Apparent Concentration	Weight %	Atomic %	Apparent Concentration	Weight %	Atomic %
BTO-NFO	Ba	7.60	36.03	8.28	9.09	40.19	10.41
	Ti	3.11	14.18	9.35	2.85	12.12	9.00
	Ni	0.93	4.38	2.36	1.46	6.46	3.91
	Fe	1.39	6.82	3.86	2.06	9.44	6.01
	O	8.43	38.59	76.15	7.72	31.78	70.66
Total		100.00			100.00		

V. VSM ANALYSIS:

The Magnetization field-dependent curve is taken at room temperature (300 K) and it is observed that the composite has a superparamagnetic behavior within the soft ferromagnet with negligible coercivity and remanence magnetization with the absence of hysteresis loop [10,35]. Magnetic coercivity H_C, retentivity M_r and saturation magnetization M_S analyzed from the hysteresis, are tabulated and further the Mr/Ms ratio is calculated. From the table it is observed that on increasing the soft side content, coercivity, retentivity and saturation magnetization increases.

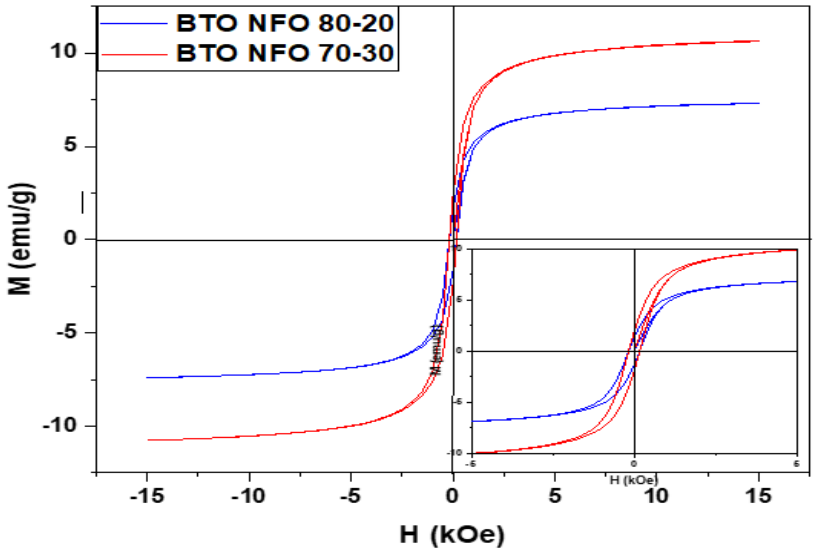

Table 4. M_r, M_s, H_c and M_r/M_s ratio values for BTO-NFO 80-20 and 70-30 nanocomposites.

Sample	M_r (emu/g)	M_s (emu/g)	H_c (kOe)	M_r/M_s
BTO-NFO 80-20	1.6628	7.35433	0.17631	0.22609845
BTO-NFO 70-30	2.39392307	10.71538	0.17730	0.22341000

The maximum retentivity 2.39 emu/g and saturation magnetization, 10.71 emu/g is obtained for BTO-NFO 70-30 nanocomposites. The coercivity of both samples are almost negligible which states that there exists a superparamagnetic state within the ferromagnetic sample.

The obtained Ms is applicable for various biological applications like drug delivery, hyperthermia, MRI, etc. The ratio Mr/Ms is known as the squareness ratio and it measures how square the hysteresis loop is. i.e. it is the characteristic parameter of the magnetic materials and provides information by which the direction of magnetization orients to the nearest easy axis magnetization direction after the magnetic field is switched off. The squareness ratio for the prepared sample is much less than 0.5, which states that multidomain grains or single domains are formed and the particle interaction is by magneto-static interaction confirming its superparamagnetic nature. It is important to note that such magnetic behavior is observed at just 0.1 % concentrations on both hard and soft sites of the nanocomposite.

VI.CONCLUSION:

A novel low temperature cost effective simple technique was employed to successfully synthesize pure Barium Titanate - Nickel ferrite nanocomposites. Since both preparation methods have control over their particle size, smaller particles of 10 nm can be synthesized for various nano applications. The main aim of this work is to analyze the magnetic moment, Spectroscopic and Optical bandwidth of the nanocomposites for novel magnetic and optical applications. Based on the results, the composites have better Structural, morphological and optical properties compared to other oxide-based nanocomposites. It is important to note that such magnetic and optical behavior is observed at just 0.1 % concentrations on both hard and soft sites of the nanocomposite.

The obtained low Ms values and Mr/Ms ratio are applicable for various biological applications like drug delivery, hyperthermia, MRI, etc.

DECLARATION OF COMPETING INTEREST

The authors declare that they have no known competing financial interests or personal relationships that could have appeared to influence the work reported in this paper.

ACKNOWLEDGEMENT

We, the authors are thankful to our President, Chancellor, Chief Executive Officer, Vice Chancellor and Registrar of Karpagam Academy of Higher Education, Coimbatore, India for providing facilities and encouragement. Our thanks are also due to Sophisticated Analytical Instrument Facility (SAIF) for VSM Analysis.

REFERENCE

1. D. Zhang et al., “Magnetic-field-induced dielectric behaviors and magneto-electrical coupling of multiferroic compounds containing cobalt ferrite/barium calcium titanate composite fibers,” Journal of Alloys and Compounds, vol. 740, pp. 1067–1076, Apr. 2018, doi: 10.1016/J.JALLCOM.2018.01.081.
2. L. Lin, H. Ning, S. Song, C. Xu, and N. Hu, “Flexible electrochemical energy storage: The role of composite materials,” Composites Science and Technology, vol. 192, p. 108102, May 2020, doi: 10.1016/J.COMPSCITECH.2020.108102.
3. R. Samad, M. ud D. Rather, K. Asokan, and B. Want, “Magneto-dielectric studies on multiferroic composites of Pr doped CoFe2O4 and Yb doped PbZrTiO3,” Journal of Alloys and Compounds, vol. 744, pp. 453–462, May 2018, doi: 10.1016/J.JALLCOM.2018.01.403.
4. M. Vijatovic Petrovic, J.D. Bobic, and B.D. Stojanovic, Magnetic, Ferroelectric, and Multiferroic Metal Oxides , vol. Metal Oxides. Amsterdam: Elsevier Publisher, 2018.

5. A. Jain, A. K. Panwar, A. K. Jha, and Y. Sharma, "Improvement in dielectric, ferroelectric and ferromagnetic characteristics of Ba0.9Sr0.1Zr0.1Ti0.9O3-NiFe2O4 composites," Ceramics International, vol. 43, no. 13, pp. 10253–10262, Sep. 2017, doi: 10.1016/J.CERAMINT.2017.05.053.
6. R. J. Pandya, U. S. Joshi, and O. F. Caltun, "Microstructural and Electrical Properties of Barium Strontium Titanate and Nickel Zinc Ferrite Composites," Procedia Materials Science, vol. 10, pp. 168–175, Jan. 2015, doi: 10.1016/J.MSPRO.2015.06.038.
7. Y. Wang et al., "An extremely low equivalent magnetic noise magnetoelectric sensor," Advanced Materials, vol. 23, no. 35, pp. 4111–4114, Sep. 2011, doi: 10.1002/adma.201100773.
8. Y. Wang et al., "Ultralow equivalent magnetic noise in a magnetoelectric Metglas/Mn-doped Pb(Mg 1/3Nb 2/3)O 3-PbTiO 3 heterostructure," Applied Physics Letters, vol. 101, no. 2, Jul. 2012, doi: 10.1063/1.4733963.
9. Z. Chu et al., "A 1D Magnetoelectric Sensor Array for Magnetic Sketching," Advanced Materials Technologies, vol. 4, no. 3, Mar. 2019, doi: 10.1002/admt.201800484.
10. M. J. PourhosseiniAsl et al., "Versatile power and energy conversion of magnetoelectric composite materials with high efficiency via electromechanical resonance," Nano Energy, vol. 70, Apr. 2020, doi: 10.1016/j.nanoen.2020.104506.
11. J. Zhai, S. Dong, Z. Xing, J. Li, and D. Viehland, "Giant magnetoelectric effect in Metglas/polyvinylidene-fluoride laminates," Applied Physics Letters, vol. 89, no. 8, 2006, doi: 10.1063/1.2337996.
12. Y. H. Chu et al., "Electric-field control of local ferromagnetism using a magnetoelectric multiferroic," Nature Materials, vol. 7, no. 6, pp. 478–482, 2008, doi: 10.1038/nmat2184.
13. J. M. Hu, Z. Li, L. Q. Chen, and C. W. Nan, "High-density magnetoresistive random access memory operating at ultralow voltage at room temperature," Nature Communications, vol. 2, no. 1, 2011, doi: 10.1038/ncomms1564.
14. A. Kumar, S. H. Kim, M. Peddigari, D. H. Jeong, G. T. Hwang, and J. Ryu, "High Energy Storage Properties and Electrical Field Stability of Energy Efficiency of (Pb0.89La0.11)(Zr0.70Ti0.30)0.9725O3 Relaxor Ferroelectric Ceramics," Electronic Materials Letters, vol. 15, no. 3, pp. 323–330, May 2019, doi: 10.1007/s13391-019-00124-z.
15. H. Wu, A. Tatarenko, M. I. Bichurin, and Y. Wang, "A multiferroic module for biomechanical energy harvesting," Nano Energy, vol. 83, May 2021, doi: 10.1016/j.nanoen.2021.105777.
16. S. Hajra, V. Vivekananthan, M. Sahu, G. Khandelwal, N. P. M. Joseph Raj, and S. J. Kim, "Triboelectric nanogenerator using multiferroic materials: An approach for energy harvesting and self-powered magnetic field detection," Nano Energy, vol. 85, Jul. 2021, doi: 10.1016/j.nanoen.2021.105964.
17. G. Liu et al., "Ultrahigh dielectric breakdown strength and excellent energy storage performance in lead-free barium titanate-based relaxor ferroelectric ceramics via a combined strategy of composition modification, viscous polymer processing, and liquid-phase sintering," Chemical Engineering Journal, vol. 398, Oct. 2020, doi: 10.1016/j.cej.2020.125625.
18. H. Chandrasekar, T. Razzak, C. Wang, Z. Reyes, K. Majumdar, and S. Rajan, "Demonstration of Wide Bandgap AlGaN/GaN Negative-Capacitance High-Electron-Mobility Transistors (NC-HEMTs) Using Barium Titanate Ferroelectric Gates," Advanced Electronic Materials, vol. 6, no. 8, Aug. 2020, doi: 10.1002/aelm.202000074.
19. K. Gireesh Baiju, B. Murali, and D. Kumaresan, "Ferroelectric barium titanate microspheres with superior light-scattering ability for the performance enhancements of flexible polymer dye sensitized solar cells and photodetectors," Solar Energy, vol. 224, pp. 93–101, Aug. 2021, doi: 10.1016/j.solener.2021.05.063.
20. T.-H. Vu, N. T. M. Phuong, and T. Nguyen, "Lead-free ferroelectric barium titanate -based thin film for tunable microwave device application," IOP Conference Series: Materials Science and Engineering, vol. 1091, no. 1, p. 012060, Feb. 2021, doi: 10.1088/1757-899x/1091/1/012060.
21. Tiening Jin and P. Lin, "Efficient Mid-Infrared Electro-Optical Waveguide Modulators Using Ferroelectric Barium Titanate," IEEE Journal of Selected Topics in Quantum Electronics, pp. 1–7, 2020.
22. C. Zhai, H. Zhang, L. Du, D. Wang, D. Xing, and M. Zhang, "Nickel/iron-based bimetallic MOF-derived nickel ferrite materials for triethylamine sensing," CrystEngComm, vol. 22, no. 7, pp. 1286–1293, Feb. 2020, doi: 10.1039/c9ce01807g.
23. V. Manikandan et al., "Effect of Vd-doping on dielectric, magnetic and gas sensing properties of nickel ferrite nanoparticles," Journal of Materials Science: Materials in Electronics, vol. 31, no. 19, pp. 16728–16736, Oct. 2020, doi: 10.1007/s10854-020-04228-3.
24. T. Adinaveen, P. Leema Sophie, D. Santhanaraj, and M. Amalraj, "Role of Mg2+ substitution on viscosity and thermal conductivity of nickel ferrite based magnetic fluids," Journal of Dispersion Science and Technology , Feb. 2021.
25. S. L. Pereira, H.-D. Pfannes, A. A. Mendes Filho, L. C. B. de M. Pinto, and M. A. Chíncaro, "A comparative study of NiZn ferrites modified by the addition of cobalt," Materials Research, vol. 2, no. 3, pp. 231–234, 1999, doi: 10.1590/s1516-14391999000300020.
26. M. Athika, V. S. Devi, and P. Elumalai, "Cauliflower-Like Hierarchical Porous Nickel/Nickel Ferrite/Carbon Composite as Superior Bifunctional Catalyst for Lithium-Air Battery," ChemistrySelect, vol. 5, no. 12, pp. 3529–3538, Mar. 2020, doi: 10.1002/slct.202000013.
27. E. Samuel, A. Aldalbahi, M. El-Newehy, H. El-Hamshary, and S. S. Yoon, "Nickel ferrite beehive-like nanosheets for binder-free and high-energy-storage supercapacitor electrodes," Journal of Alloys and Compounds, vol. 852, Jan. 2021, doi: 10.1016/j.jallcom.2020.156929.
28. H. J. Kardile, S. B. Somvanshi, A. R. Chavan, A. A. Pandit, and K. M. Jadhav, "Effect of Cd2+ doping on structural, morphological, optical, magnetic and wettability properties of nickel ferrite thin films," Optik, vol. 207, Apr. 2020, doi: 10.1016/j.ijleo.2020.164462.

AUTHORS PROFILE

Ashwin Sudhakaran, Research Scholar Department of Physics, Karpagam Academy of Higher Education, Coimbatore-641021, Tamilnadu, India. Phone: +91 9003995469. Email ID: dr.ashwinsudhakar@gmail.com. ORCID ID: https://orcid.org/0000-0001-7408-5711

Allwin Sudhakaran, Research Scholar Department of Physics, Karpagam Academy of Higher Education, Coimbatore-641021, Tamilnadu, India. Phone: +91 9500439546. Email ID: dr.allwinsudhakar@gmail.com. ORCID ID: https://orcid.org/0000-0001-6361-7364

Dr. E. Sivasenthil, Associate Professor, Department of Physics, Karpagam Academy of Higher Education, Coimbatore-641021, Tamilnadu, India. Phone: +91 9842950616. Email ID: sivasenthil.e@kahedu.edu.in. ORCID ID: : https://orcid.org/0000-0002-2302-4748